NASA TECHNICAL MEMORANDUM

NASA TM X- 71423

NASA TM X- 71423

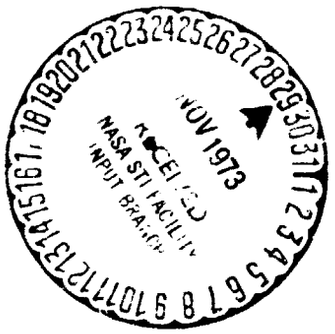

THERMODYNAMICS AND KINETICS OF PACK ALUMINIDE COATING FORMATION ON IN-100

by S. R. Levine and R. M. Caves
NASA - Lewis Research Center
U.S. Army Air Mobility Research and Development Laboratory
Cleveland, Ohio 44135

TECHNICAL PAPER proposed for presentation at
144th National Meeting of the Electrochemical Society
Boston, Massachusetts, October 7 - 12, 1973

THERMODYNAMICS AND KINETICS OF PACK ALUMINIDE COATING FORMATION ON IN-100

by S. R. Levine and R. M. Caves

National Aeronautics and Space Administration
Lewis Research Center
Cleveland, Ohio

ABSTRACT

An investigation of the effects of pack variables on the formation of aluminide coatings on nickel-base superalloy IN-100 was conducted. Also, the thermodynamics and kinetics of coating formation were analyzed. Observed coating weights were in good agreement with predictions made from the analysis. Pack temperature rather than pack aluminum activity controls the principal coating phase formed. In 1 weight percent aluminum packs, aluminum weight gains were related to the halide pack activator as follows: $F \simeq Cl > Br > I$. Solid-state nickel diffusion controlled coating formation from sodium fluoride and chloride and ammonium fluoride activated packs. In other ammonium and sodium halide activated 1 weight percent aluminum packs, gaseous diffusion controlled coating formation.

E-7678

SUMMARY

The effect of variation of pack activators, compositions, temperature, and time on the thickness and structure of aluminide coatings formed on the nickel-base superalloy IN-100 was studied in one-step packs containing aluminum at unit activity. Times were varied from 4 to 24 hours and temperatures were varied from 982° to 1149° C in NaCl activated packs. The other halides of sodium and the ammonium halides were primarily used to activate 1093° C, 16-hour packs.

In addition, an analysis of the thermodynamics and kinetics of alu-

minizing was carried out. The mechanism of coating formation in each pack was established from agreement between observed coating weights and predictions based on a gaseous diffusion model and published diffusion data for the Ni-Al system. Pack temperature rather than pack aluminum activity controls the principal coating phase formed.

The halides ranked according to aluminum weight gain in 1 weight percent Al packs are F ≅ Cl > Br > I. Solid-state nickel diffusion controlled the rate of coating formation in fluoride activated packs. Gaseous diffusion controlled the rate of coating formation in 1 weight percent Al bromide and iodide and NH_4Cl activated packs. In NaCl activated packs containing 1 weight percent Al the ability of the substrate to supply nickel appeared to be in balance with the ability of the pack to supply aluminum. However, the observed rate constant and activation energy indicated that solid-state diffusion controlled.

Increasing pack aluminum content from 1 to 5 weight percent shifted control of coating formation from the gas phase to the solid-state in the 16-hour, 1093° C NaBr activated pack.

Regardless of the rate controlling step, the kinetics of coating formation were parabolic. The activation energy for coating formation controlled by solid-state diffusion was 88 kcal/mole.

Similar coating microstructures and weight gains were obtained for each halogen regardless of whether its source was a sodium or ammonium halide.

INTRODUCTION

Aluminide coatings are commonly used to extend the life of superalloys in the oxidation/corrosion/erosion environment encountered in gas

turbines (1). Such protection is provided by aluminum oxide scales which preferentially form on the β-NiAl phase which is analogous to NiAl in the Ni-Al binary system. Generally these intermetallic aluminide coatings are diffusion formed by exposing the blade or vane alloy surface to an aluminum-rich environment at elevated temperature. The aluminides may be applied by a number of methods including pack cementation, slurry spraying and sintering, and slurry spraying and fusing in the presence of a fluxing agent (2,3). The pack cementation method is the most established and commonly used technique for large scale batch processing of engine components currently in commercial flight service.

Although the commercial pack aluminides are performing successfully in the 700° to 1000° C metal operating temperature range of current engines, the requirements of higher operating temperatures for improved engine performance with even longer times between overhaul will place ever more stringent demands on coating technology. Even if new coating systems come into use for these high-temperature needs, the relatively low cost aluminide coatings will continue to be used at peak temperatures to 1100° C. One way to improve such aluminide coatings is by gaining a more thorough understanding of the pack cementation process and then using this insight to optimize pack conditions for each alloy and application.

A fairly extensive background on pack aluminizing exists in the literature, but knowledge of the effect of pack variables on coating structure and performance remains far from complete (2,4-6). Goward and Boone (5) have summarized the formation mechanisms for aluminide coatings. They formulate two classifications:(1) the low-temperature, high-

activity pack and (2) the high-temperature, low-activity pack. Each coating class has its peculiarities and advantages. The two step high-activity process (application followed by diffusion annealing) tends to first form M_2Al_3 which reverts to MAl on annealing. Such coatings incorporate substrate constituents and microstructural features, whereas the low-activity process (which also may require two steps) tends to form MAl and to incorporate only selected substrate constituents (4). In the high-activity process, aluminum is supplied at a rate much greater than it can react to form β-NiAl. Thus Ni_2Al_3 is formed by :d diffusion of Al. In the low-activity process the rate of supply of aluminum is less than the rate at which nickel can be supplied through β and thus nickel-rich β is formed. The advantages derived from each pack class might be conferred upon a coating by a one-step hybrid pack in which aluminum is present at unit activity and the temperature is high enough to maintain β formation.

The purpose of this study was to develop a fuller understanding of the important processing variables, transport mechanisms, and thermodynamics of the pack aluminizing process. This was done by studying the effect of several pack activators, pack compositions, temperatures, and times on the thickness and structure of pack aluminide coatings formed on nickel-base superalloy IN-100 in high-activity, high-temperature hybrid packs.

Prior exploratory studies evolved a pack consisting of 1 weight percent NaCl, 1 weight percent Al with the balance inert Al_2O_3 filler to which the substrates are exposed for 16 hours at 1093° C under an argon atmosphere. In this study the fluorides, chlorides, bromides, and iodides of sodium and ammonium were used as activators. Pack times were varied

from 3 to 24 hours, pack temperatures were varied from 982° to 1149° C, and activator and aluminum concentrations were varied over the range of 1 to 3 and 1 to 5 weight percent, respectively.

The coated specimens were evaluated by weight gain, optical metallography, microhardness measurements, electron microprobe raster micrography (EMP), X-ray fluorescence (XRF), and X-ray diffraction (XRD).

EXPERIMENTAL PROCEDURES

Coating Deposition

Commercially cast IN-100 having a nominal composition of 5.5 w/o Al, 15.3 w/o Co, 9.6 w/o Cr, 3.2 w/o Mo, 4.3 w/o Ti, 0.9 w/o V, 0.17 w/o C, with the balance nickel and minor trace elements was the substrate used for this study. Specimens were cast in two configurations: 5.1 × 2.5 × 0.25 cm coupons and 10.2 × 2.5 × 0.44 cm erosion bars. Specimen edges were radiused to 0.04 to 0.08 cm by abrasive tumbling or grinding on a water-wetted belt sander. Both types of specimens were then grit blasted with -100 mesh Al_2O_3 to produce a uniform matte finish, rinsed, measured, vapor degreased, rinsed in distilled water and weighed prior to placement in the pack.

The pack box consisted of an aluminized Inconel retort as shown in cross section in Figure 1. The specimens were rested in a premixed powder consisting of Alcoa A-1 grade -100 mesh alumina powder, -100 mesh 99 percent pure Al and reagent grade activator salt. The packs contained at least 1 weight percent Al and 1 weight percent activator. The balance was Al_2O_3. In one NaI activated pack the activator content was raised to 3 weight percent and in one NaBr activated pack the aluminum content was raised to 5 weight percent.

The assembled pack was purged for one hour with high purity argon prior to insertion into the preheated box furnace which was controlled to $\pm 15^{\circ}$ C. The packs required about one hour to heat up to the furnace temperature. Pack times are reported as time at temperature rather than as time in the furnace. Argon flow was maintained at 0.057 m^3/hr throughout the time the packs were above room temperature. Upon completion of the scheduled exposure, the pack was removed from the furnace and cooled to room temperature. The specimens were removed from the powder, brushed, rinsed in distilled water, and weighed to determine aluminum pick-up.

Additional Evaluations

Metallographic cross sections of some specimens in the as-coated condition were examined to evaluate the effect of the various pack conditions on coating structure and thickness. In addition, microhardness measurements were made with a Knoop indentor driven by a 200 gram load. EMP analyses by electron back scatter and element X-ray raster micrography were performed on some metallographic cross sections of the coated specimens to determine qualitative element distributions. Also, XRF analyses in situ and XRD analyses of scrapings and in situ were performed.

The pack materials from completed 16 and 24 hour, 1093° C, NaCl activated packs were analyzed for Cl, Na, and Al. Three bulk samples from the 24-hour pack were leached to extract the following elements: one sample was water leached to extract Cl and Al present as soluble halide salt; another was HCl leached to extract Na and Al; and a third was given a redundant NaOH leach to check the extraction of Cl and Al. Na was analyzed by flame emission spectroscopy, Al was determined by atomic absorption spectroscopy, and Cl was determined by spectrophotometry using the

mercuric thiocyanate procedure. Sequential leaches on single samples were used to analyze a bulk sample and a sample taken from within 0.5 cm of the specimen surface in the 16-hour pack.

RESULTS

The results of aluminide coating deposition on IN-100 in packs activated with the halides of sodium and ammonium are presented in Table I.

Effect of Time in Chloride Activated Packs

Coating deposition times of 4, 8, 16, and 24 hours at 1093° C were used with the baseline NaCl activated pack. As shown in Table I, the scatter within a pack was generally small. However, there was more variation in coating weight and thickness between packs as primarily observed in the 16-hour packs. This variation influenced coating composition and microstructure. A satisfactory explanation for this behavior could not be found. Variations in temperature; variable levels of residual oxygen, nitrogen and moisture in the assembled packs, or incomplete mixing of the pack ingredients may be responsible.

XRD analysis indicated that the coatings deposited by 1093° C NaCl activated packs were primarily β-MAl. Ni_2Al_3 was detected in situ as a minor coating phase in a coating put down in 8 hours and in the heaviest coating put down in 16 hours.

Photomicrographs of coatings deposited by the NaCl activated packs are presented in Figure 2. The zone adjacent to the substrate which etched distinctly lighter in the 4, 8, and 16 hour pack coatings is of relatively constant thickness (16 to 30 micrometers) as a function of time compared to the growth of the outer or primary coating layer (32 to 77 micrometers). In all coatings a discontinuous layer of carbides sim-

ilar in appearance to the substrate carbides was clearly visible in the as polished samples. The samples coated for 4 and 8 hours have microstructures characteristic of "low-activity" pack coatings with carbides concentrated in the light etching zone adjacent to the substrate (5). In the samples aluminided for longer times the carbides also penetrate the primary layer. Some substrate carbide depletion (not shown) was noticeable after 16 hours. After 24 hours the thickness of the substrate carbide depleted zone was comparable to the coating thickness. Since the carbides in the coating are rich in Ti, Mo, and V as were the substrate carbides, they are presumed to be of the MC type (7). Their distribution and the occurrence of carbide depletion of the substrate indicates formation of these carbides in the coating by precipitation as well as by inclusion as a result of coating growth. An additional minor coating phase, revealed as the light etching particles concentrated primarily in the lighter etching zone, is rich in Cr, Mo, and V and lean in Ni, Co, and Ti. Occasional Al_2O_3 inclusions (large dark particles) and other particles (primarily rich in Cr) are also found in the primary layer.

The coating deposition data for NaCl activated packs, as plotted in figure 3, were fit to power law growth equations

$$x = (kt)^{1/n}; \qquad w = (k't)^{1/n'} \tag{1}$$

appropriate for diffusion through a growing phase or depleting zone in the pack. Analysis of thickness (x) and weight (w) data gave $1/n$ and standard deviation values of 0.54 ± 0.10 and 0.56 ± 0.12 for thickness and weight data, respectively, indicating parabolic behavior. Fitting the thickness data to a parabolic growth equation ($n = 2$) gives a rate constant (k) of $1.6\times10^{-}$ cm^2/sec with a standard deviation of $\pm0.4\times10^{-9}$ cm^2/sec.

The data for NH_4Cl activated packs, as plotted in Figure 3, were fit to the power law growth equation. Using the standard deviations found for NaCl, the values of 1/n and their standard deviations are 0.46±0.10 and 0.49±0.12 for thickness and weight gain data, respectively. These values suggest that parabolic kinetics prevailed in NH_4Cl activated packs. The parabolic rate constant was $1.3\pm0.4\times10^{-9}$ cm^2/sec (again using the standard deviation obtained for NaCl.

Effect of Time - NaBr Activated Packs

Microstructures of coatings deposited in 4, 8, 16, and 24-hour 1 weight percent aluminum Nabr activated 1093° C packs are presented in Figure 4. The outer inclusion free zone of the coatings deposited in 4, 8, and 16 hour packs shows a transition in etching behavior as a function of depth not seen in coatings deposited in NaCl activated packs. This is indicative of a transition from Al-rich MAl at the surface to Al-lean MAl in the coating interior. (4). The interface between the inclusion-free outer zone and the inner zone is quite irregular in NaBr activated packs when compared to the interface developed in NaCl activated packs (Fig. 2). This irregularity is indicative of sensitivity to small local variations in pack composition as previously reported by Brill-Edwards and Epner (6).

The aluminum weight gain data are plotted against pack time in Figure 5. When fit to the power law rate equation, 1/n and standard deviation values of 0.44±0.13 and 0.44±0.04 were obtained for thickness and weight gain data, respectively. Thus coating formation adheres fairly well to a parabolic growth law. The parabolic rate constant was 7.9×10^{-10} cm^2/sec with a standard deviation of $\pm2.3\times10^{-10}$ cm^2/sec. This is less than the parabolic rate constants calculated for coating formation

in chloride activated packs. The differences in rate constants, coating microstructures, and sensitivities to local variations in pack composition between coatings formed in chloride and bromide activated packs may be indicative of a difference in the rate controlling step in coating formation in these packs.

Effect of Temperature

Coating deposition temperatures of 982° , 1038° , 1093° , and 1149° C were used with NaCl activated packs run for 16 hours. Inclusion of data from 15-hour 1093° C packs is felt to introduce a negligible error. The log of coating weight squared at constant time is, to a good approximation, a linear function of reciprocal absolute temperature as can be seen from Figure 6. A +15° C variation in temperature gives an ±8% increase in coating thickness. Regression analyses of weight gain and coating thickness data for assumed parabolic behavior gave activation energies of 88 Kcal/mole. The standard deviations of the activation energy (slope) were ±11 and ±13 Kcal/mole for the lines fit to thickness and weight data, respectively.

XRD results confirmed that the primary coating phase was β. Photomicrographs of coatings deposited at each of the four pack temperatures are shown in Figure 7. Coatings deposited at 982° through 1093° C are very similar in general microstructure. They all have the characteristic inclusion-free outer or primary β layer and a distinctly defined, lighter etching zone having a high concentration of MC carbide inclusions. Second phase inclusions are concentrated at the inner part of the primary layer in the 982° and 1038° C deposited coatings as they were in the coating applied in the 8-hour 1093° C pack. Longer times or higher tempera-

tures spread the distribution of these particles throughout the outer layer. The growth of the primary β layer was much more sensitive to temperature than was the growth of the secondary zone adjacent to the substrate. Carbide depletion of the substrate to a depth comparable to the coating thickness (not shown), recrystallization of the columnar secondary zone, formation of a layer of γ (nickel solid solution) at the coating substrate interface and growth of a zone of large equiaxed grains essentially free of second phase inclusions in the outer β layer have all occurred in the coating deposited at 1149° C. The coating is also considerably softer than coatings deposited at lower temperatures. These features are characteristic of a partially depleted aluminide coating on IN-100 (8). In summary, coating microstructures obtained in 982° or 1038° C 16-hour packs (Fig. 7(a,b)) and 1093° C 4 and 8-hour packs (Fig. 2(a,b)) have microstructures characteristic of low-activity pack coatings (i.e., a single phase β outer coating zone) whereas the coating microstructures obtained at higher temperatures or longer times are hybrids incorporating features found in heat treated high-activity pack coatings and low-activity pack coatings as discussed by Goward and Boone (5).

Effect of Activators

The results of activator variation in 16-hour 1093° C packs are listed in Table I and plotted as bar graphs in Figure 8(a,b). In all cases XRD analysis of the coatings detected β as the major coating phase. Examination of Figure 8(a,b) indicates that aluminum pick-up generally increases with decreasing atomic number of the halogen. XRF analyses of the surface (Fig. 8(c,d)) indicated that the trend for sur-

face nickel content was approximately the inverse of the trend for aluminum pick-up; i.e., surface nickel content generally increased with increasing atomic number of the halogen. These observations indicate that the ability of higher molecular weight halogens to deposit aluminum is less than that of lower molecular weight halogens. Thus gas phase kinetics and thermodynamics must play a significant role in aluminum deposition under some conditions.

The changes in halide and the accompanying changes in the rate of coating formation have an effect on the coating microstructure and phase distribution as can be seen in the photomicrographs in Figures 9 and 10. The coatings formed in 16-hour fluoride and chloride activated packs have microstructural features derived from both the heat treated high-activity and the low-activity pack classifications. The bromide and iodide activatated pack coatings (Figs. 9(c,d) and 10(c,d)) have microstructural features peculiar to low-activity pack coatings. Aluminum content in these coatings is generally lower than in lower temperature or shorter time NaCl activated pack coatings having about the same weight (Figs. 3(a,b) and 7(b)). Consequently, the coatings formed in bromide and iodide activated packs are generally softer than coatings formed in corresponding fluoride and chloride activated packs. However, they have microstructures similar to these NaCl activated pack coatings.

Effect of Pack Composition

An increase in pack aluminum and NaCl content from 1 to 2% had no significant impact on aluminum pick-up in a 1093° C, 16-hour pack. Also, an increase in NaI content from 1 to 3% had no significant impact on aluminum deposition in a 1093° C, 16-hour, 1% aluminum pack. However, an

increase of aluminum content from 1 to 5% in a 1% NaBr, 1093° C, 16-hour pack increased aluminum pick-up from 6.8 to 16.1 mg/cm^2. The microstructure of this coating, shown in Figure 11, is very similar to microstructures of 16 and 24-hour NaCl deposited coatings. This sensitivity to pack aluminum content indicates that gas phase kinetics play a significant role in the rate of aluminum deposition in NaBr activated packs. Similar behavior could be anticipated in NH_4Br and iodide activated packs based on the strong similarities between coatings put down by these packs and the 1 weight % Al, NaBr activated pack.

DISCUSSION

Pack Stability

In this study aluminide coatings were deposited on IN-100 in a semi-open system. The ability of such a system to maintain stable bulk pack aluminum deposition capability throughout an experiment is a natural first subject for discussion. For example, a maximum in coating microhardness was observed at 16 hours and Ni_2Al_3 was detected as a minor phase only in 8- and 16-hour coatings deposited in 1093° C, NaCl activated packs. These observations may be indicative of a decline in bulk pack aluminum deposition capability with time or may merely be due to the growth of a depleted zone in the pack adjacent to the specimen surface.

To obtain some feeling for the stability of the various packs and eventually permit an analysis of the kinetics of aluminum deposition, thermodynamic analyses for the initial bulk pack compositions were performed. The results of the thermodynamic analyses of the bulk pack compositions, as discussed in detail in appendix A, are presented in Table II. On the basis of condensed phases present, the packs fall into

three groups: sodium halide activated packs with NaX(l) and Al(l) present; NH_4F activated packs with AlF_3(s) and AlN(s) present; and NH_4X (X = Cl, Br or I) activated packs with Al(l) and AlN(s) present. Based on the nature of the condensed phases present at local equilibrium in the bulk pack as listed in Table II, the sodium halide and ammonium fluoride activated packs should be stable as a function of time whereas the other ammonium halide activated packs may not be stable.

The results of Cl, Na, and Al analyses of pack material from a 24-hour NaCl activated 1093° C pack as listed in Table III did not confirm that a significant decrease in bulk pack aluminum deposition capability occurred. Calculation of the partial pressures of reactive species in the pack at 24 hours from the results of the chemical analyses gave values equal to or greater than those calculated for the initial conditions. Thus the absence of Ni_2Al_3 in the 24-hour pack is attributed to formation of a depleted zone in the pack at the specimen surface. More direct evidence of depleted zone formation was obtained from XRD and chemical analyses of samples taken from the bulk pack and from within 0.5 cm of the sample surface after completion of a 16-hour, 1093° C NaCl activated pack as reported in Table III. Aluminum was detected by XRD as a minor phase in the bulk pack but was not detected at the specimen surface. Conversely, NaCl was detected as a possible minor phase at the specimen surface but was not detected in the bulk pack. Chemical analyses of these samples, as listed in Table III, confirm the XRD results. The Al content of the bulk pack was considerably higher than that of the pack close to the specimen surface whereas the Na and Cl constants of the bulk pack were found to be lower than at the specimen surface. Thus a depleted zone is formed in

the packs. Formation of a depleted zone in aluminiding packs was previously reported by Brill-Edwards and Epner (6). An idealized sketch of the depleted zone is shown in Figure 12. The actual depleted zone probably does not show an abrupt transition since gaseous diffusion permits gradual depletion of aluminum over an extended transition zone.

Since no condensed halide source is present in NH_4X (X = Cl,Br,I) activated packs whereas NaX(1) is present in corresponding sodium halide packs the stability of the NH_4X packs may be considerably lower than that of NaX activated packs. Also, for example, extremely high initial deposition rates may be obtained with NH_4Cl during the early part of the coating cycle when the partial pressure of AlCl(g) is more than an order of magnitude higher than in the NaCl activated pack. However, the coating deposition data for NaCl and NH_4Cl activated packs, plotted in Figure ?, suggest that the NH_4X (X = Cl, Br, or I) activated packs behave similarly to NaX activated packs in the sense that initial deposition rates are not significantly different and that rapid dilution of the NH_4Cl activated pack does not occur in spite of the absence of a condensed halide phase. In addition, there is strong correspondence between the microstructures and weights of coatings applied by corresponding halides of sodium and ammonium as can be seen from Figures 9 and 10 and Table I.

Pack Kinetics - Experimental

In this study parabolic rate constants of $1.3\pm0.4\times10^{-9}$ cm^2/sec for NH_4Cl activated coating deposition and $1.6\pm0.4\times10^{-9}$ cm^2/sec for NaCl activated coating deposition were obtained. These values are less than rate constants reported by Janssen and Rieck (9) for growth of NiAl between

Ni_2Al_3 and Ni_3Al and for nonstoichiometric NiAl from NiAl and Ni. Extrapolation of their results to 1093° C gave rate constants of 5×10^{-9} cm^2/sec for the former reaction and 6×10^{-9} cm^2/sec for the latter. The difference between rate constants for coating formation on IN-100 and diffusion in binary couples could be due to both the effects of solutes such as Cr, Co, and Ti derived from the IN-100 substrate and to the order of magnitude variation in diffusivity between stoichiometric NiAl (in which the diffusivity of nickel is a minimum) and nickel-rich NiAl (10) (which controls layer growth as determined by Janssen and Rieck).

Also, in this study an activation energy of 88±13 Kcal/mole was obtained for the deposition process in NaCl activated packs. This value is in poor agreement with a value of 41 Kcal/mole reported by Janssen and Rieck (9) for diffusion of nickel in β as determined by layer growth studies. However, the activation energy falls close to the upper end of the range of values for nickel diffusion in NiAl reported by Hancock and McDonnell (10): 73.4±2.3Kcal/mole for stoichiometric NiAl to 42.5±6.3 Kcal/mole for the 48.3 atom % Ni composition. The activation energy is also in agreement with the activation energy of 81 Kcal/mole reported for Co diffusion in NiAl by Berkowitz et al. (11). Based on the coating growth rate constants and activation energies observed in this study and their reasonable agreement with data for the NiAl system (9-11), we conclude that nickel diffusion through the coating may be the rate controlling step in NaCl and NH_4Cl activated packs run between 982° and 1149° C. Additional support comes from metallography and XRD results which indicated that the coating was primarily β and from the observed insensitivity of NaCl packs to 1% variations in aluminum and activator content.

In NaBr activated packs high sensitivity of coating weight to pack aluminum content was observed. The kinetics of aluminum deposition in 1 weight % NaBr packs adhered reasonably well to a parabolic growth law, but the parabolic rate constant ($7.9\pm2.3\times10^{-10}$ cm^2/sec) was smaller than in NaCl activated packs ($1.6\pm0.4\times10^{-9}$ cm^2/sec). Based on the sensitivity of NaBr packs to aluminum content and the lower aluminum pick-up of 1 wt % Al bromide and iodide activated packs compared to chloride and fluoride activated packs, the authors conclude that gas phase kinetics was the rate controlling step in aluminum deposition from bromide and iodide activated packs containing 1 wt % aluminum.

Pack Kinetics - Analytical

To further elucidate the role of gas phase kinetics in aluminide coating formation, analyses of aluminum transport from the bulk pack through the pack depleted zone to the surface of the coating were carried out. The starting points for the analyses were the thermodynamic calculations discussed in appendix A and the pack depletion zone model, Figure 12. The analyses of gas phase kinetics are discussed in appendix B where the calculation of instantaneous fluxes of aluminum for a simplified case is outlined. The instantaneous flux is given by

$$\frac{N_{Al}d}{A} = \frac{\sum_{i=1}^{n} D_i(P_i - P_i')}{RT} \qquad (2)$$

where D_i and P_i are the diffusivity and partial pressure of the i^{th} aluminum bearing species with the prime referring to the sample surface and d is the diffusion distance. The computations included mass balances on H, X, and Na and allowed for condensation of NaX(1) as appropri-

ate. In NH_4X activated packs dilution by 9.8 moles of argon (4 hr of argon flow) was used to arrive at bulk pack compositions. In the case of NH_4F pseudo-equilibrium bulk pack compositions were used since dilution with 9.8 moles of argon results in disappearance of the $AlF_3(s)$ phase. The computations were made for an assumed surface aluminum activity of 1×10^{-2}. This is a reasonable choice for average aluminum activity in view of the fact that Steiner and Komarek (12) report an activity of 1×10^{-2} for aluminum in stoichiometric NiAl at 1000° C. Results are listed in table IV for major diffusing species.

From the instantaneous fluxes the diffusion direction of each species in the pack depleted zone was ascertained. These are illustrated in Figure 13 for (a) the simplified model for NaX activated packs in which NaX(1) condensation was not considered, (b) the complete model for NaX activated packs where NaX(1) condensation was considered and (3) for NH_4X activated packs. Instantaneous fluxes of major species are compared to the net instantaneous aluminum flux in Figure 14. Aluminum is deposited primarily by AlX. NaX(1) condensation (Fig. 14(b)) augments aluminum deposition by not requiring halogen removal by AlX_2 and AlX_3 diffusion (Fig. 14(a)). In reality, the actual fluxes for NaX activated packs are probably bounded by the complete and simplified models. Evidence of NaX condensation in the depleted zone was obtained. However, some depletion of Na as a result of reaction with alumina and by transport out of the semi-open system does occur.

Computed instantaneous fluxes were relatively insensitive to changes in assumed surface aluminum activity. A tenfold decrease in surface aluminum activity increased the computed flux by only a factor of 2.

In addition to aluminum being deposited, loss of substrate species from IN-100 can contribute to observed net specimen weight change and thus cause misinterpretation of coating weight. Analyses were performed for Ni and Cr. Very small amounts of nickel are lost from the substrate as nickel and nickel halide. At 1366° K the partial pressure of nickel over the alloy is only about 10^{-10} atm (13). This gives a nickel flux of about 10^{-14} moles/cm^2-sec from the coating surface to the bulk pack.

The estimated Cr partial pressure over IN-100 is 0.1 $P_{Cr} = 1.3\times10^{-7}$ atm at 1366°K (13). This gives a Cr flux of about 1.3×10^{-11} moles/cm^2-sec. Thus, at worst, the chromium weight loss in a 16-hour 1093° C pack was about 1% of the aluminum weight gain.

The rate of aluminum deposition dw/dt in mg/cm^2-sec was computed from the instantaneous fluxes according to the following equation:

$$\frac{dw}{dt} = \left(\frac{\rho}{w}\right)\left(\frac{\epsilon}{l}\right)(m_{Al}1000)\left(\frac{N_{Al}^{d}}{A}\right) \qquad (3)$$

The term $\frac{\rho}{w} = \frac{1}{d}$ defines the growth of the pack depleted zone in terms of coating weight w and pack aluminum content $\rho = 8$ mg/cm^3 in 1 wt % Al packs. The term ϵ/l corrects for diffusion through a porous medium. The effective transport area of the pack is to a good approximation, equal to the pack porosity $\epsilon = 0.79$. In addition, the transport path is non-linear and a correction factor $l = 4$ was arbitrarily assumed. The third term converts from moles of aluminum to milligrams. Integration gives:

$$w^2 = \frac{2\rho\epsilon}{l}\left(\frac{N_{Al}^{d}}{A}\right) 2.7\text{x}10^4\ t \qquad (4)$$

The aluminum deposition rate constants

$$k_{Al} = \frac{2\rho\epsilon}{l}\left(\frac{N_{Al}^{d}}{A}\right) 2.7\text{x}10^4 \qquad (5)$$

are listed in Table IV. Inclusion of sodium halide condensation results in a 1.7 to 11-fold increase in k_{Al} depending on the halide. The moles of NaX(1) condensed are about equal to the moles of Al deposited according to the complete solution.

Predicted aluminum weight gains for 16-hour 1 weight % Al packs are also listed in Table IV. These predicted values are plotted against observed aluminum weight gains in Figure 15. For NaX activated packs an average predicted value was used. The good agreement between observed and predicted coating weights in bromide and iodide activated 1 weight % Al packs confirms that deposition is controlled by gaseous diffusion. The choice of an ℓ value of 5 would have given better agreement. Earlier it was stated that solid-state diffusion of nickel may be the rate controlling step in NaCl and NH_4Cl activated packs. However, good agreement between observed and predicted weights based on the gaseous diffusion model indicates that gaseous diffusion controls coating deposition in NH_4Cl activated packs. There appears to be a balance between the predicted ability of the pack to supply aluminum and the observed ability of the substrate to absorb aluminum via nickel diffusion in NaCl activated packs. However, in 1 wt % Al packs activated with NaCl, based on the observed rate constant and activation energy the solid-state diffusion step can be considered rate controlling. If gaseous diffusion was rate controlling a pseudo-activation energy of 50 Kcal/mole would have been observed rather than 88 Kcal/mole. Similarly, in the 5 wt % Al pack activated with NaBr the agreement between observed and predicted coating weights based on the gaseous diffusion model is good. However, based on coating weight and microstructure, the solid-state diffusion step can be

considered rate controlling.

In fluoride activated packs predicted coating weights based on gaseous diffusion models were 2 to 5 times greater than observed weights. The net aluminum deposition rate constants for assumed parabolic behavior, when put on a thickness basis (using a conversion factor of 7.7×10^{-4} cm/mg/cm^2), were 1.0×10^{-8} and 4.8×10^{-8} cm^2/sec for the NH_4F and NaF activators, respectively. These rate constants are greater than rate constants for NiAl growth as determined from Janssen and Rieck (9) by more than an order of magnitude. Thus, a posteriori, solid-state diffusion controls the rate of coating growth when the net aluminum deposition rate constant is greater than 5×10^{-9} cm^2/sec (8.4×10^{-3} mg^2/cm^4-sec) at 1093° C in the Ni-Al system. Since observed coating weights were limited to 15.3±3.3 mg/cm^2, solid state diffusion controls deposition on IN-100 when the net aluminum deposition rate constant exceeds $4.3\pm1.8\times10^{-3}$ mg^2/cm^4-sec or $2.5\pm1.1\times10^{-9}$ cm^2/sec. Predicted coating weights for fluoride activated packs are plotted on a solid state diffusion control basis in Figure 15.

CONCLUDING REMARKS

In this experimental and analytical study of high-temperature packs having aluminum present at unit activity, MAl coating formation was controlled by either solid-state or gaseous diffusion. Although the experiments were performed on IN-100, the analysis is quite general and may be applied to any nickel-base superalloy. Based on these results it appears that the classification of aluminide packs into "high-activity" and "low-activity" as proposed by Goward and Boone (5) is misleading. Coating formation can be more accurately described in terms of the ability of the

pack to supply aluminum and the ability of the substrate to supply nickel. The primary variable is temperature rather than pack aluminum activity. This is illustrated in Figure 16 where the classifications proposed by Goward and Boone are shown on the left. Coatings similar to those produced in low-activity packs can be produced in packs having aluminum present at unit activity provided that they are carried out at high-temperature as illustrated on the right of Figure 16. The coating formation process can be controlled either by diffusion in the gas phase or solid phase depending upon the activator and pack aluminum content.

SUMMARY OF RESULTS

The effect of variation of pack activators, pack compositions, temperature, and time on the thickness and structure of aluminide coatings formed on nickel-base alloy IN-100 was studied in a series of one-step packs in which aluminum was initially present at unit activity. Times were varied from 4 to 24 hours and temperatures were varied from 982° to 1149° C in NaCl activated packs. The other halides of sodium and the ammonium halides were primarily used to activate 1093° C, 16-hour packs. Through an analysis of the thermodynamics and kinetics of reactions in the pack and comparison with published diffusion data in the Ni-Al binary system the mechanism of coating formation in each pack was established. The following are the results of this study:

1. Coating weights can be successfully predicted from analyses of pack thermodynamics and diffusion in the pack and coating.

2. Pack temperature rather than pack aluminum activity controls the principal coating phase formed.

3. The halide pack activators ranked in order of decreasing aluminum

weight gain in 1 weight % aluminum packs are: $F \doteq Cl > Br > I$.

4. Solid state nickel diffusion was the rate controlling step in coating formation in fluoride activated packs. Gaseous diffusion controlled the rate of coating formation in 1 weight % Al bromide and iodide activated packs and NH_4Cl activated packs. In NaCl activated packs containing 1 weight % Al the predicted ability of the pack to supply aluminum was in balance with the ability of the substrate to supply nickel. However, the observed rate constants and activation energy indicated that the solid-state diffusion step controlled coating growth.

5. An increase in pack aluminum content from 1 to 5 weight % shifted control of coating formation from gas phase diffusion to solid-state diffusion in 16-hour, 1093° C NaBr packs and resulted in a coating similar in weight, thickness, and microstructure to those formed in NaCl activated packs.

6. Regardless of the rate controlling step, the kinetics of coating formation were near parabolic.

7. The activation energy for coating formation controlled by solid-state diffusion was 88±13 Kcal/mole on IN-100.

8. Similar coating microstructures and weight gains were obtained for each halogen regardless of whether its source was a sodium or ammonium salt. Coating microstructures bore greatest resemblance to "low-activity" pack coatings with some features peculiar to "high-activity" pack coatings apparent in coatings applied for longer times or at higher temperatures.

APPENDIX A

THERMODYNAMICS

Calculation of bulk pack composition at equilibrium was accomplished with the aid of CEC 71, a computer program by Gordon and McBride described in NASA SP-273 (14). The thermodynamic data for the program were taken from the JANAF tables (15). Data for NaI(g), which were not available in the JANAF tables, were computed from spectrochemical data by B. J. McBride, Lewis Research Center (private communication). Pack compositions prior to establishment of equilibrium were computed from the pack starting materials.

To illustrate the calculation, the outline of an approximate hand calculation method for sodium halide activated packs follows:

1. Chemical reactions

$$3NaX(l) + Al(l) = AlX_3(g) + 3Na(g) \tag{A1}$$

$$Al(l) + 2AlX_3(g) = 3AlX_2(g) \tag{A2}$$

$$Al(l) + AlX_2(g) = 2AlX(g) \tag{A3}$$

$$Na(g) + X(g) = NaX(l) \tag{A4}$$

2. Equations

a. Sodium balance:

$$M_{NaX(g)} + M_{Na(g)} + M_{NaX(l)} = M^{o}_{NaX(s)} \tag{A5}$$

b. Halogen balance:

$$M_{X(g)} + M_{NaX(g)} + M_{NaX(l)} + 3M_{AlX_3(g)} + 2M_{AlX_2(g)} + M_{AlX(g)} = M^{o}_{NaX(s)} \tag{A6}$$

c. Equilibrium - equation (1):

$$K_3 = P^3_{Na} P_{AlX_3} \tag{A7}$$

d. Equilibrium - equation (2):

$$K_2 = \frac{P_{AlX_2^3}}{P_{AlX_3^2}} \tag{A8}$$

e. Equilibrium - equation (3):

$$K_1 = \frac{P_{AlX^2}}{P_{AlX_2}} \tag{A9}$$

f. Equilibrium - equation (4):

$$K_4 = \frac{1}{P_{Na} P_X} \tag{A10}$$

Elimination of $M^o_{NaX(c)}$ between equations (5) and (6) permits the resulting equation to be rewritten in terms of pressures. This leaves five equations in five unknowns. The solution was performed for NaF and NaCl activators. The results agreed with the computer program to within 20 percent for the former and 3 percent for the latter. The difference was primarily due to exclusion of minor species in the hand calculation. Results of the computer solutions are listed in Table II. In one case, the NaF activated pack, the presence of Al_2O_3 was included in the machine calculations. The species present at equilibrium were Al(l), Al, AlF, AlF_2, AlF_3, AlO, AlOF, Al_2F_6, Al_2O, Al_2O_2, Al_2O_3(S), Ar, F, Na, NaF(l), NaF, NaO, Na_2, and Na_2F_2. No significant difference in the partial pressures of F, AlF, AlF_2, and AlF_3 were noted when the results were compared with the calculation made with Al_2O_3 omitted. Thus Al_2O_3 was omitted from all other calculations. One shortcoming of the analysis of the NaF activated pack should be noted: cryolite formation was not considered. Since the cryolite melt is extensively dissociated (18) the impact of cryolite formation on this analysis is considered small.

PPENDIX B

KINETICS

Instantaneous fluxes of gaseous species from the bulk pack to the substrate surface and vice versa were computed for 1 atmosphere total pressure and a surface aluminum activity of 1×10^{-2}. The results are summarized in Table IV. Several checks on diffusion conditions were made prior to performing the calculation. First, it was established that diffusion occurs in the viscous flow regime. For molecular diffusion to occur the pack particle size would have to be reduced from about 100 microns to about 0.1 micron. Second, it was established that interchange between argon and hydrogen occurs very rapidly in the NH_4F activated pack and therefore diffusivities were computed based on argon as the major constituent. The computation was performed for equilibrium conditions after dilution by 9.8 moles of argon in NH_4Cl,Br and I activated packs and pseudo-equilibrium conditions in NH_4F activated packs. Diffusivities were estimated from the Gilliland equation (16):

$$D = \frac{0.0043\left[T^3\left(\frac{1}{m_a} + \frac{1}{m_b}\right)\right]^{1/2}}{P\left(V_a^{1/3} + V_b^{1/3}\right)^2} \qquad \text{(B1)}$$

Molar volumes at the normal boiling point were computed from data in the literature (17) and from an estimated value of 18 cm^3/gm-atom for aluminum.

In making the instantaneous flux calculations the roles of $Na_i(g)$ and NaX in sodium halide activated packs and of HX(g) and $H_2(g)$ in NH_4X activated packs were included. Solution of this problem involving as many as ten simultaneous equations was accomplished on a digital computer.

The instantaneous flux calculation in outline form for a simplified case for NaX activated packs wherein the roles of $Na_i(g)$ and NaX are neglected follows:

1. Chemical reactions

   a. Bulk pack

$$Al(l) + X(g) = AlX_1(g) \tag{B2}$$

$$Al(l) + 2X(g) = AlX_2(g) \tag{B3}$$

$$Al(l) + 3X(g) = AlX_3(g) \tag{B4}$$

   b. Surface

      Substitute Al (Al in NiAl) for Al(l) in equations (2), (3), and (4).

2. Equilibrium equations

   a. Equation (2):

$$K_1 = \frac{P_X(g)a_{Al}}{P_{AlX_1}(g)} = \frac{P_4 a}{P_1} \tag{B5}$$

   b. Equation (3):

$$K_2 = \frac{P^2_{X(g)}a_{Al}}{P_{AlX_2}(g)} = \frac{P^2_4 a}{P_2} \tag{B6}$$

   c. Equation (4):

$$K_3 = \frac{P^3_{X(g)}a_{Al}}{P_{AlX_3}(g)} = \frac{P^2_4 a}{P_3} \tag{B7}$$

For reactions in the bulk pack the aluminum activity is set equal to $P_{Al(g)}/P_{Al(l)} = 1$. For reactions at the surface aluminum activity was set at $1 \cdot 10^{-2}$ and the pressures are distinguished by primes.

3. Instantaneous fluxes:

a. Aluminum to the surface:

$$\frac{N_{Al}}{A} = \frac{D_1}{RT}\frac{(P_1 - P_1')}{d} + \frac{D_2}{RT}\frac{(P_2 - P_2')}{d} + \frac{D_3}{RT}\frac{(P_3 - P_3')}{d} \qquad (8)$$

The contribution of Al(g) diffusion to the net aluminum flux is negligible.

b. Halogen balance at the surface:

$$0 = D_1(P_1 - P_1') + 2D_2(P_2 - P_2') + 3D_3(P_3 - P_3') + D_4(P_4 - P_4') \qquad (9)$$

The unknowns are P_1', P_2', P_3', P_4', N_{Al}/A and d. Multiplication of both sides of equation (8) by d gives the combined variable $N_{Al}d/A$ and leaves five equations and five unknowns. Therefore, each pressure and the instantaneous fluxes of all species can be estimated. P_1' and the instantaneous fluxes are listed in Table IV. Instantaneous fluxes were found to be relatively insensitive to changes in surface aluminum activity. A tenfold decrease in aluminum activity increases the net instantaneous aluminum flux by a factor of 2.

APPENDIX C

NOMENCLATURE

A	area, cm^2
a	activity of aluminum at the coating surface, dimensionless
D_i	diffusivity of the i^{th} species, cm^2/sec
d	diffusion distance, cm
K_j	equilibrium constant for the j^{th} reaction
k,k'	rate constant
l	path length correction factor
M	moles
m_a,m_b	molecular weight, grams/mole
N_{Al}	aluminum flow, moles/sec at any instant
n,n'	rate equation exponent
P_i	partial pressure of the i^{th} species in the bulk pack, atm
P_i'	partial pressure of the i^{th} species at the coating surface, atm
Q	activation energy, Kcal/mole
R	gas constant, cm^3-atom/^oK-mole or cal/^oK-mole
T	absolute temperature, ^oK
t	time, sec
V_a,V_b	molar volume at the normal boiling point, cm^3/mole
w	coating weight, mg/cm^2
X	halogen atom, F, Cl, Br, or I
x	coating thickness, cm
ϵ	pack porosity
ρ	pack aluminum concentration, mg/cm^3

REFERENCES

1. Grisaffe, S.J.: "The Superalloys", Sims, C.T. and Hagel, W.C., Editors, Ch. 12, John Wiley & Sons, Inc., New York (1972).

2. Gadd, J.D ; Nejedlik, J.F.; and Graham, L.D.: Electrochem. Tech., 6, 307 (1968).

3. Stetson, A.R.: U.S. Patent 3,927,043 (1960).

4. Goward, G W ; Boone, D H.; and Giggins, C S.: Trans. ASM, 60 228 (1967).

5. Goward, G.W.; and Boone, D.H.: Oxidation of Metals, 3, 475 (1971).

6. Brill-Edwards, H.; and Epner, M.: J. Electrochem. Soc. 6, 299 (1968).

7. Collins, H.E.: Trans. ASM, 62, 82 (1969).

8. Caves, R.M.; and Grisaffe, S.J.: NASA TN D-6317 (1971).

9. Janssen, M.M.P.; and Rieck, G.D.: Trans. AIME, 239, 1372 (1967).

10. Hancock, G.F.; and McDonnell, B.R.: Phys. Stat. Sol., 4, 143 (1971).

11. Berkowitz, A.E.; Jaumot, F.E.; and Nix, F.C.: Phys. Rev., 95, 1185 (1954).

12. Steiner, A.; and Komarek, K.L.: Trans. AIME, 230, 786 (1964).

13. Weast, R.C., Editor, "Handbook of Chemistry and Physics", Chemical Rubber Co., Cleveland, Ohio (1971).

14. Gordon, S.; and McBride, B.J.: NASA SP-273 (1971).

15. Anon., "JANAF Thermochemical Tables", Dow Chemical Co., Midland, Mich. Dec. 31, 1960 to June 30, 1970.

16. Gilliland, E.R.: Ind. Eng. Chem., 26, 681 (1934).

17. LeBas: "The Molecular Volumes of Liquid Chemical Compounds", Longuens, London (1915) (Referenced in A.S. Foust, et. al.; "Principles of Unit Operations", John Wiley & Sons, Inc., New York, 1960).

18. Frank, W.B.: J. Phys. Chem., 65, 2081 (1961).

TABLE I. - PACK ALUMINIDE COATING DEPOSITION PARAMETERS AND RESULTS

Activator	Temperature, °C	Time, hr	Weight %		Aluminum pick-up, mg/cm^2	Coating thickness, μm	XRF (a)			XRD		
			Activator	Aluminum			Al	Ni	Ti	Major phase	Minor phases	
NaF	1093	16	1	1	13.3±1.2	108	6.0	64	1.3	MAl	Al_2Cr_3	Al_2O_3
NaCl	982	16	↓	↓	2.6±0.1	18	8.3	72	.2	MAl	-	-
↓	1038	16			6.0±0.6	40	9.1	72	.3	MAl	Al_2O_3	-
	1038	16			6.4±0.4	46	9.4	73	.1	MAl	-	-
	1093	4			7.4	48	-	--	-	MAl	-	-
	↓	8			7.1±0.3	50	7.1	74	0.1	MAl	Ni_2Al_3	-
		8			7.9±0.1	62	-	--	-	-	-	-
		15	2	[b]2	13.9±0.5	-	-	--	-	-	-	-
		15	1	1	12.2±0.2	79	-	-	-	MAl	-	-
		16	↓	↓	18.6±0.3	115	7.7	69	0.1	MAl	Ni_2Al_3	-
		16			15.4	-	-	-	-	-	-	-
		24			14.3±1.3	107	6.8	71	0.2	MAl	-	-
		24			17.2±0.3	115	-	-	-	-	-	-
	1149	16			16.1±3.0	132	8.5	67	0.5	MAl	Al_2O_3	-
NaBr	1093	4			3.8	35	-	-	-	MAl	-	-
↓	↓	8			5.5	48	-	-	-	MAl	-	-
		16	↓	↓	6.8±0.2	52	7.2	81	0.1	MAl	Al_2Cr_3	-
		16	1	5	16.1	136	-	-	-	MAl	-	-
		24	1	1	8.4	86	-	-	-	MAl	-	-
NaI		16	1	1	5.1±0.3	50	7.4	78	0.1	MAl	-	-
NaI		16	3	1	5.9±0.1	-	-	-	-	-	-	-
NH_4F		16	1	1	15.7±2.9	115	4.3	59	4.2	MAl	NiO	TiO_2
NH_4Cl		3	↓	↓	4.6±0.2	42	-	-	-	MAl	-	-
NH_4Cl		16			10.5±1.6	90	7.1	74	0.3	MAl	-	-
NH_4Br		16			7.6±0.1	73	5.4	81	0.1	MAl	Al_2O_3	-
NH_4I	↓	16	↓	↓	5.2±0.2	53	5.2	80	0.1	MAl	-	-

[a]Counts relative to counts from IN-100 X100.

[b]Spacing between specimens, 3.3 cm minimum except for this pack where 1.9 cm spacing was used.

TABLE II. - CALCULATED INITIAL PRESSURES OF REACTIVE PACK SPECIES (ATM)

Activator	Temperature, °C	P_{Al}	P_{AlX}	P_{AlX_2}	P_{AlX_3}	$P_{Al_2X_6}$	P_{AlH}	ΣP_{AlX_i}	P_{NaX}	$P_{Na_2X_2}$	P_{Na}	P_{Na_2}	ΣP_{Na_i}
NaF	1093	1.54×10^{-6}	8.19×10^{-2}	2.36×10^{-3}	3.61×10^{-3}	1.39×10^{-5}		8.79×10^{-2}	1.23×10^{-3}	6.20×10^{-4}	9.63×10^{-2}	6.15×10^{-4}	9.69×10^{-2}
NaCl	982	1.41×10^{-7}	9.04×10^{-4}	8.07×10^{-5}	3.81×10^{-7}	$<3\times10^{-7}$	-	9.85×10^{-4}	6.91×10^{-3}	2.48×10^{-3}	1.07×10^{-3}	1.42×10^{-7}	1.07×10^{-3}
NaCl	1038	4.96×10^{-7}	2.03×10^{-3}	1.89×10^{-4}	9.09×10^{-7}	$<3\times10^{-7}$	-	2.22×10^{-3}	1.44×10^{-2}	4.82×10^{-3}	2.41×10^{-3}	5.20×10^{-7}	2.41×10^{-3}
NaCl	1093	1.54×10^{-6}	4.20×10^{-3}	4.03×10^{-4}	1.98×10^{-6}	$<3\times10^{-7}$	-	4.61×10^{-3}	2.77×10^{-2}	8.67×10^{-3}	5.01×10^{-3}	1.66×10^{-6}	5.01×10^{-3}
NaCl	1149	4.45×10^{-6}	8.27×10^{-3}	8.20×10^{-4}	4.10×10^{-6}	$<3\times10^{-7}$	-	9.10×10^{-3}	5.10×10^{-2}	1.49×10^{-2}	9.91×10^{-3}	6.92×10^{-6}	9.91×10^{-3}
NaBr	1093	1.54×10^{-6}	1.75×10^{-3}	-	7.73×10^{-6}	-	-	1.76×10^{-3}	5.03×10^{-2}	-	1.77×10^{-3}	2.08×10^{-7}	1.77×10^{-3}
NaI	1093	1.54×10^{-6}	4.61×10^{-3}	-	1.23×10^{-8}	-	-	4.61×10^{-3}	1.32×10^{-1}	-	4.61×10^{-3}	1.41×10^{-6}	4.61×10^{-3}
NH_4F	1093	5.18×10^{-8}	2.06×10^{-2}	4.43×10^{-3}	5.05×10^{-2}	2.74×10^{-3}	7.91×10^{-8}	7.83×10^{-2}	-	-	-	-	-
NH_4Cl	1093	1.54×10^{-6}	7.65×10^{-2}	1.34×10^{-1}	1.20×10^{-2}	4.03×10^{-7}	2.15×10^{-6}	2.23×10^{-1}	-	-	-	-	-
NH_4Br	1093	1.54×10^{-6}	4.35×10^{-2}	-	1.19×10^{-1}	-	2.21×10^{-6}	1.63×10^{-1}	-	-	-	-	-
NH_4I	1093	1.54×10^{-6}	3.10×10^{-1}	-	3.74×10^{-3}	-	1.98×10^{-6}	3.14×10^{-1}	-	-	-	-	-

Activator	Temperature, °C	P_{HX}	P_H	P_{H_2}	ΣP_{H_i}	X	X_2	ΣP_{X_i}	Condensed phases				Initial conditions, moles			
									Al(l)	AlN (S)	AlF_3 (S)	NaX (l)	Al	Al_2O_3	Ar	Activator
NaF	1093	-	-	-	-	$<3\times10^{-15}$	$<10^{-20}$	1.13×10^{-15}	X			X	0.41	10.8	0.0098	0.26
NaCl	982	-	-	-	-	$<4.09\times10^{-12}$	$<10^{-15}$	4.09×10^{-12}	X			X				.19
NaCl	1038	-	-	-	-	2.05×10^{-11}	$<10^{-15}$	2.05×10^{-11}	X			X				
NaCl	1093	-	-	-	-	8.91×10^{-11}	$<10^{-15}$	8.91×10^{-11}	X			X				
NaBr	1093	-	-	-	-	3.51×10^{-10}	$<10^{-15}$	3.51×10^{-10}	X			X				
NaI	1093	-	-	-	-	1.94×10^{-8}	$<10^{-12}$	1.94×10^{-8}	X			X				.11
						2.90×10^{-6}	$<10^{-10}$	2.90×10^{-6}	X			X				.074
NH_4F	1093	2.72×10^{-4}	2.85×10^{-6}	9.07×10^{-1}	9.07×10^{-1}	8.47×10^{-15}	$<10^{-20}$	8.47×10^{-15}		X	X					
NH_4Cl	1093	5.55×10^{-4}	2.61×10^{-6}	7.60×10^{-1}	7.61×10^{-1}	1.62×10^{-9}	$<10^{-14}$	1.62×10^{-9}	X	X						.30
NH_4Br	1093	8.24×10^{-4}	2.68×10^{-6}	8.01×10^{-1}	8.02×10^{-1}	4.82×10^{-7}	$<10^{-10}$	4.82×10^{-7}	X	X						.21
NH_4I	1093	1.03×10^{-3}	2.41×10^{-6}	6.45×10^{-1}	6.46×10^{-1}	1.96×10^{-4}	8.73×10^{-8}	1.96×10^{-4}	X	X						.11
																.076

TABLE III. - RESIDUAL ACTIVITY OF 16- AND 24-HOUR

1093° C NaCl ACTIVATED PACKS

Chemical Analysis				
Sample	Leach	Na, ppm	Cl, ppm	Al, ppm
#1, 24-hour, bulk	H_2O		237	53
	HCl	113		2072
	NaOH		226	1995
Average values		113	232	[b]2034
#2, 24-hour, bulk	H_2O		230	33
	HCl	54		947
	NaOH		227	963
Average values		54	229	[b]955
16-hour, bulk	H_2O	31	220	0
	HCl	57	-	7540
Total values (a)		88	220	7540
16-hour, surface	H_2O	88	327	0
	HCl	55	-	360
Total values (a)		143	327	360

X-Ray Diffraction			
	Major phase	Minor phase	Possible minor phase
16-hour, bulk	α-Al_2O_3	Al	
16-hour, surface	α-Al_2O_3		NaCl

[a]Leaches were successive on a simple sample.

[b]Average Al analysis for HCl and NaOH leaches only.

TABLE IV. - MAJOR INSTANTANEOUS FLUXES AND NET ALUMINUM DEPOSITION RATE CONSTANTS AND WEIGHTS FOR GASEOUS DIFFUSION FROM A BULK 1 WT % Al PACK TO A SURFACE AT ALUMINUM ACTIVITY 1×10^{-2}

Activator	Temperature, °K	AlX				AlX_2		AlX_3		X		Na		Al_2X_6		HX		H_2		k_{Al}, $\frac{mg^2}{cm^4-sec}$	Predicted Al weight gain, mg/cm^2
		P_{1g}	P_{1S}	D_1, $\frac{cm^2}{sec}$	$\frac{D_1\Delta P_1}{RT}$, $\frac{moles-cm}{cm^2-sec}$	D_2	$\frac{D_2\Delta P_2}{RT}$	D_3	$\frac{D_3\Delta P_3}{RT}$	D_4	$\frac{D_4\Delta P_4}{RT}$	D_5	$\frac{D_5\Delta P_5}{RT}$	D_6	$\frac{D_6\Delta P_6}{RT}$	D_7	$\frac{D_7\Delta P_7}{RT}$	D_8	$\frac{D_8\Delta P_8}{RT}$		
		A. Simplified Model: Only AlX, AlX_2, AlX_3, and X considered																			
NaF	1366	8.19×10^{-2}	8.23×10^{-3}	1.57	1.0×10^{-6}	1.32	-2.6×10^{-10}	1.16	-3.4×10^{-7}	2.95	-2.7×10^{-19}									5.9×10^{-2}	5.8
NaCl	1255	9.04×10^{-4}	8.15×10^{-4}	1.12	7.5×10^{-9}	.875	-3.1×10^{-9}	.739	-3.8×10^{-10}	1.60	-1.4×10^{-15}									3.2×10^{-4}	4.3
NaCl	1311	2.03×10^{-3}	4.74×10^{-4}	1.19	1.7×10^{-8}	.934	-7.2×10^{-9}	.788	-8.4×10^{-10}	1.71	-7.2×10^{-15}									7.8×10^{-4}	6.7
NaCl	1366	4.20×10^{-3}	8.73×10^{-4}	1.27	3.8×10^{-8}	.993	-1.6×10^{-8}	.839	-1.8×10^{-9}	1.82	-3.1×10^{-14}									1.6×10^{-3}	9.7
NaCl	1422	8.27×10^{-3}	1.89×10^{-3}	1.35	7.5×10^{-8}	1.05	-3.1×10^{-8}	.891	-3.7×10^{-9}	1.93	-1.3×10^{-13}									3.2×10^{-3}	14
NaBr	1366	1.75×10^{-3}	3.66×10^{-4}	1.11	1.4×10^{-8}	-	-	.732	-4.7×10^{-9}	1.41	-5.0×10^{-12}									7.8×10^{-4}	6.7
NaI	1366	4.61×10^{-3}	4.13×10^{-3}	.981	4.1×10^{-9}	-	-	.636	-5.0×10^{-10}	1.17	-2.7×10^{-9}									3.2×10^{-4}	4.3
		B. Complete Solution: All species considered																			
NaF	1366	8.19×10^{-2}	3.00×10^{-3}	1.57	1.1×10^{-6}	1.32	2.4×10^{-8}	1.16	1.9×10^{-8}	2.95	-7.8×10^{-20}	1.93	1.2×10^{-6}	0.801	7.5×10^{-11}					1.0×10^{-1}	76
NaCl		4.20×10^{-3}	1.09×10^{-4}	1.27	4.7×10^{-8}	.993	3.4×10^{-9}	.839	1.2×10^{-11}	1.82	-2.3×10^{-15}	1.93	5.3×10^{-8}	.610	5.9×10^{-20}					4.3×10^{-3}	16
NaBr		1.75×10^{-3}	3.94×10^{-5}	1.11	1.7×10^{-8}	-	-	.732	4.4×10^{-11}	1.41	-3.1×10^{-13}	1.93	1.7×10^{-8}	-	-					1.5×10^{-3}	9.5
NaI		4.61×10^{-3}	9.18×10^{-5}	.981	4.1×10^{-8}	-	-	.636	6.6×10^{-14}	1.17	-3.0×10^{-11}	1.93	4.1×10^{-8}	-	-					3.5×10^{-3}	14
NH_4F	1366	2.06×10^{-2}	1.01×10^{-3}	1.57	2.7×10^{-7}	1.32	4.1×10^{-8}	1.16	-1.0×10^{-7}	2.95	-8.8×10^{-19}	-	-	0.801	-8.1×10^{-9}	2.61	-5.9×10^{-9}	8.17	3.1×10^{-9}	1.7×10^{-2}	31
NH_4Cl		1.27×10^{-2}	2.27×10^{-4}	1.27	1.4×10^{-7}	.993	-7.2×10^{-8}	.839	3.7×10^{-10}	1.82	-3.4×10^{-15}	-	-	.610	5.0×10^{-17}	-	-	-	-	3.5×10^{-3}	15
NH_4Br		8.34×10^{-3}	6.82×10^{-4}	1.11	7.5×10^{-8}	-	-	.732	-2.4×10^{-8}	1.41	-8.4×10^{-12}	-	-	-	-	2.29	-2.2×10^{-9}	8.17	1.1×10^{-9}	4.3×10^{-3}	16
NH_4I		7.57×10^{-3}	6.19×10^{-3}	.981	1.2×10^{-8}	-	-	.636	-1.7×10^{-9}	1.17	-4.1×10^{-9}	-	-	-	-	1.09	-3.1×10^{-9}	8.17	1.6×10^{-9}	8.9×10^{-4}	7.2

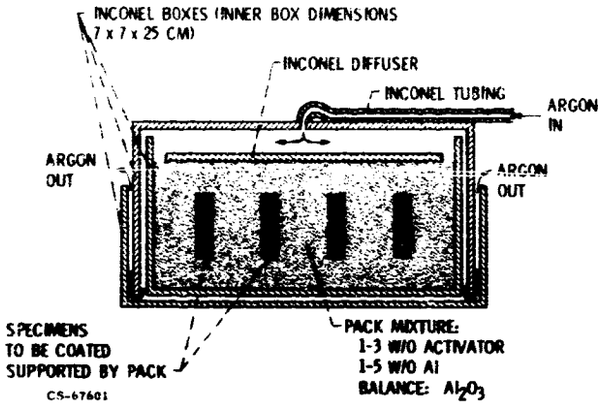

Figure 1. - Schematic cross section view of an assembled pack box.

E-7678

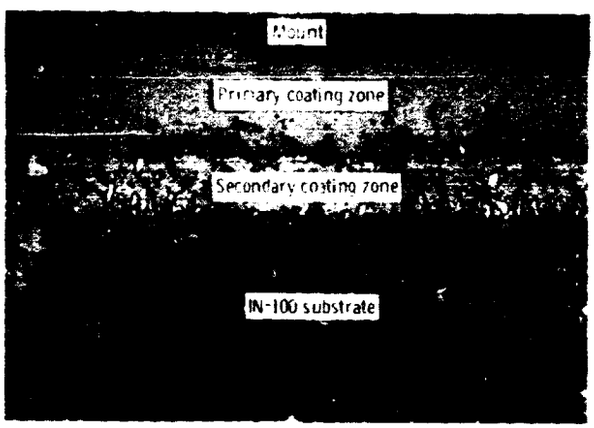

(a) 4 Hour pack.

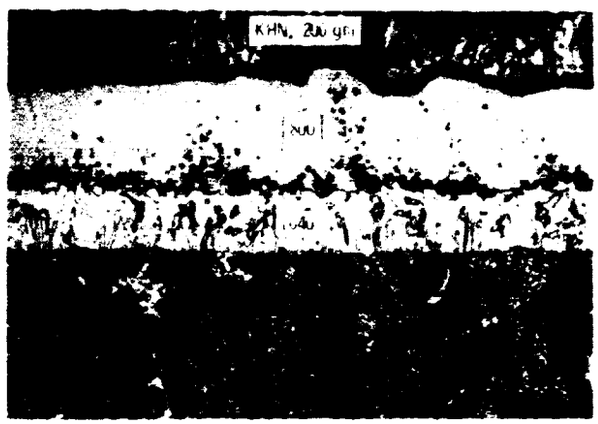

(b) 8 Hour pack.

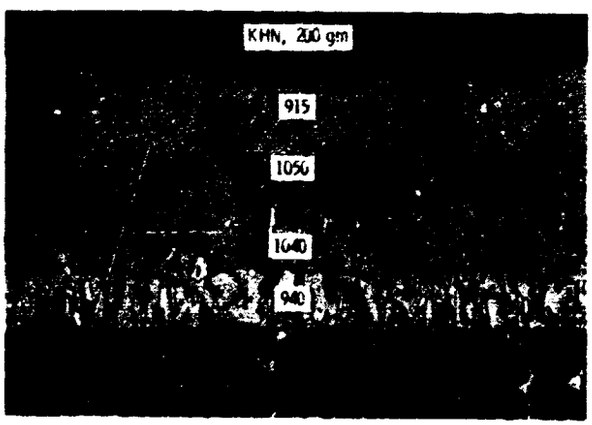

(c) 16 Hour pack.

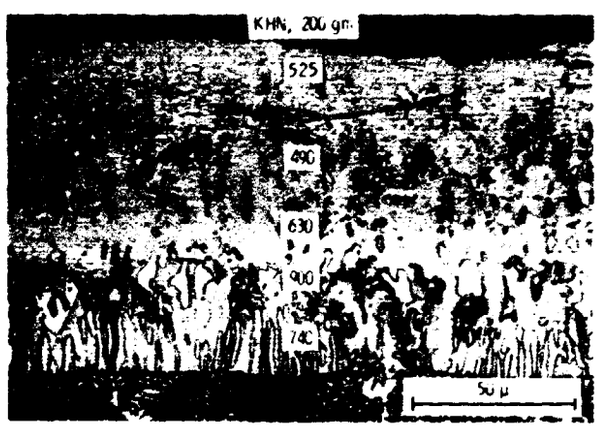

(d) 24 Hour pack.

Figure 2. - Cross sectional microstructures of aluminide coatings deposited on IN-100 in 1093° C NaCl activated packs.

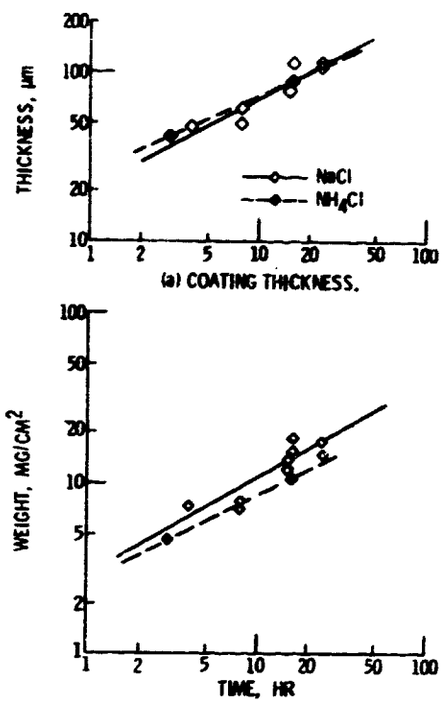

Figure 3. - Growth of aluminide coatings on IN-100 in sodium and ammonium chloride activated 1093° C packs.

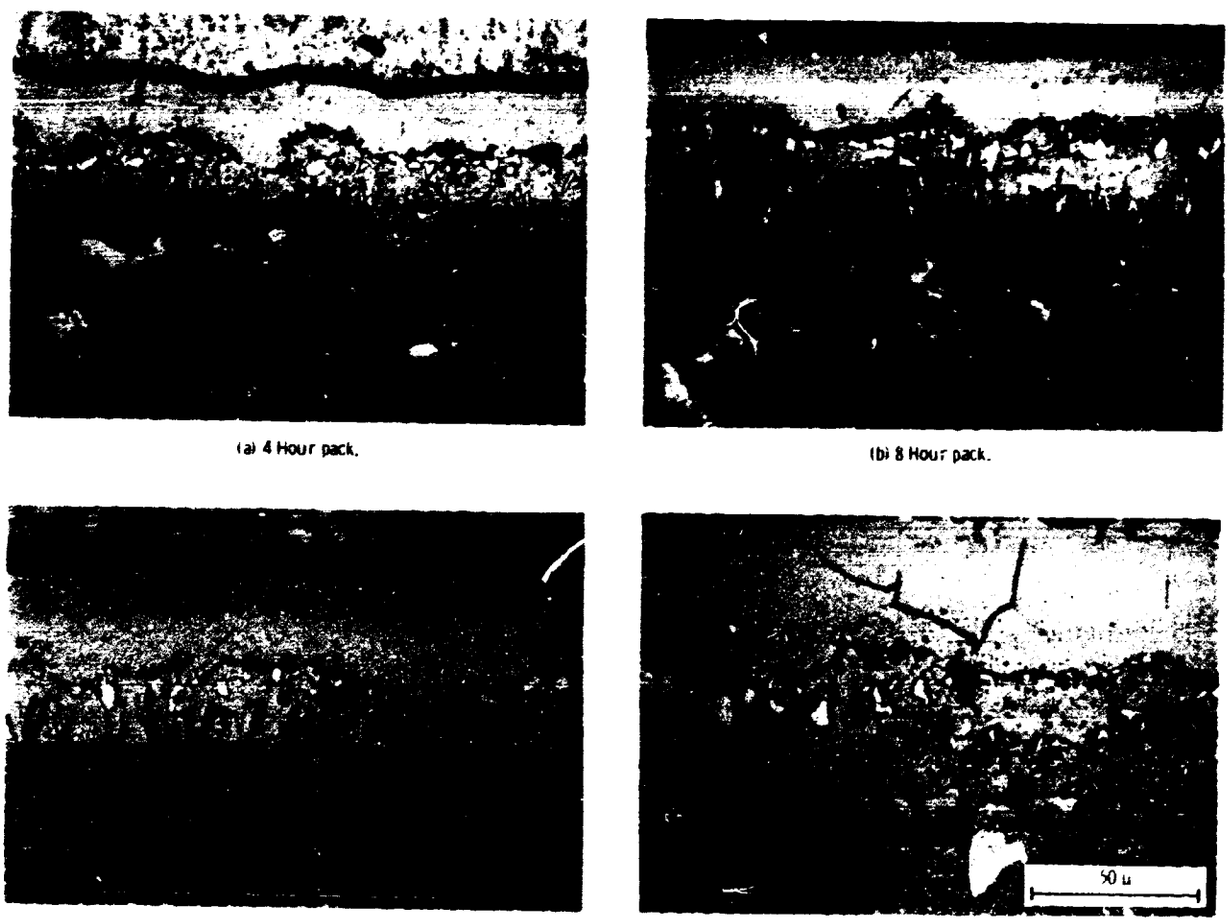

(a) 4 Hour pack.

(b) 8 Hour pack.

(c) 16 Hour pack.

(d) 24 Hour pack.

E-7678

Figure 4. - Cross sectional microstructures of aluminide coatings deposited on IN-100 in 1093° C NaBr activated packs.

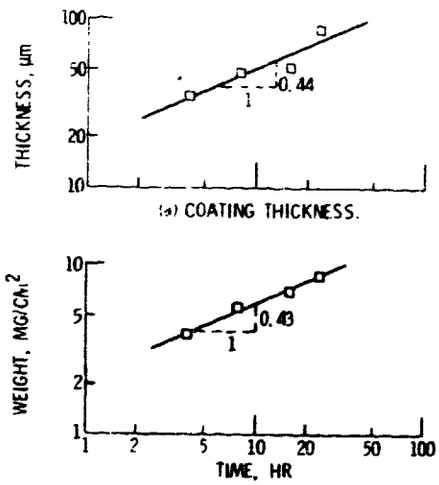

Figure 5. - Growth of aluminide coatings on IN-100 in 1 weight percent aluminum sodium bromide activated 1093° C packs.

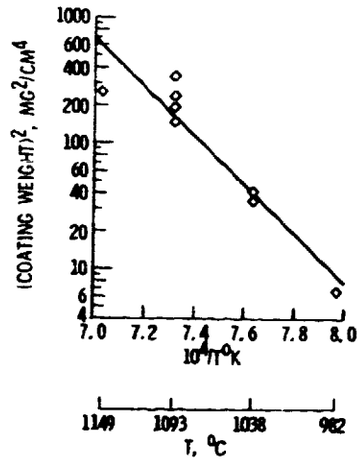

CS-67605

Figure 6. - Effect of temperature on the formation of aluminide coatings on IN-100 in 15-and 16-hour NaCl activated packs. $w^2 = kt \exp(-1000\ Q/RT)$.

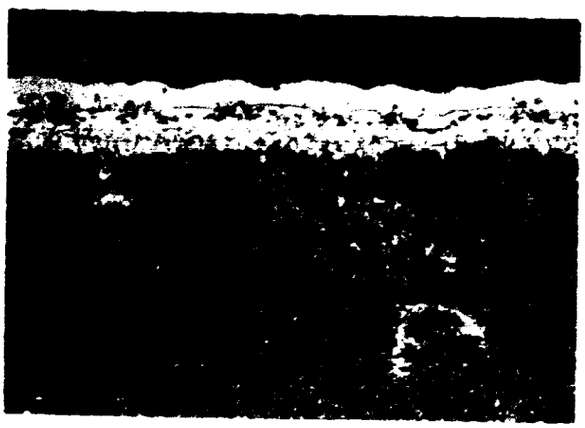

(a) 982° C pack.

(b) 1038° C pack.

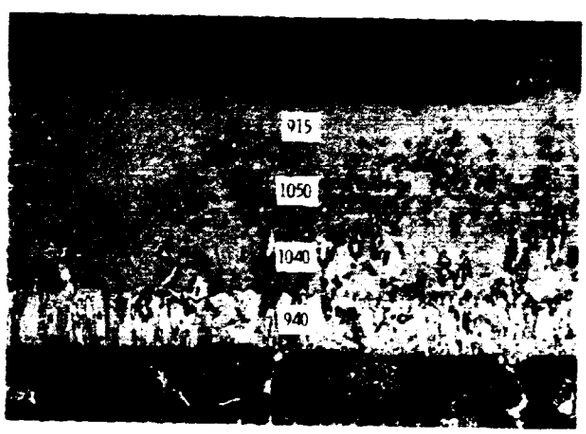

(c) 1093° pack.

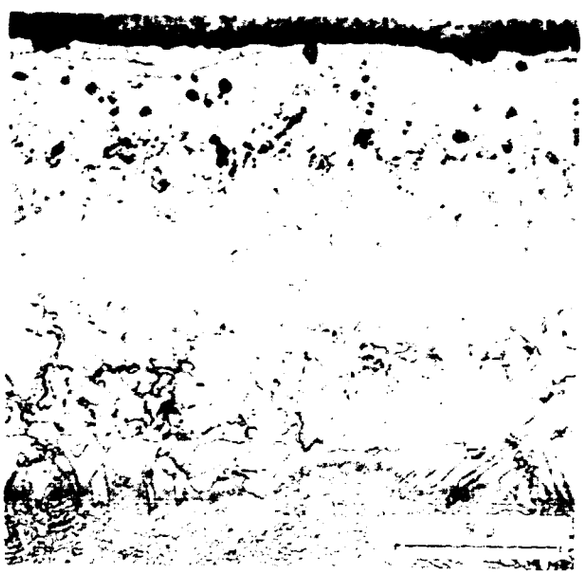

(d) 1149° pack.

E-7678

Figure 7. -Cross sectional micrographs showing the effect of temperature on aluminide coating growth on IN-100 in NaCl activated 16-hour packs.

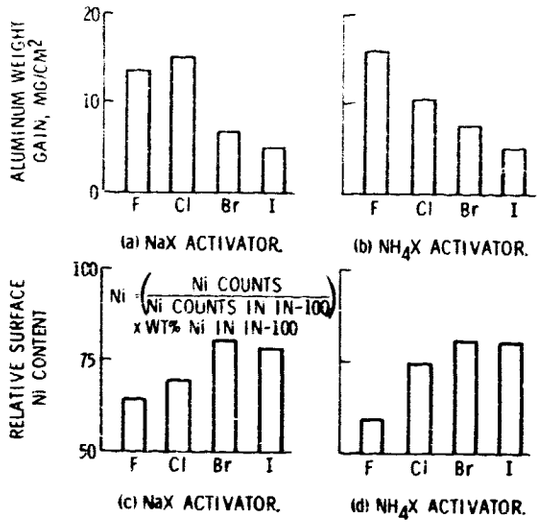

Figure 8. - Aluminum weight gain and surface nickel content in 16 hour, 1093° C packs as a function of halide activator.

E-7678

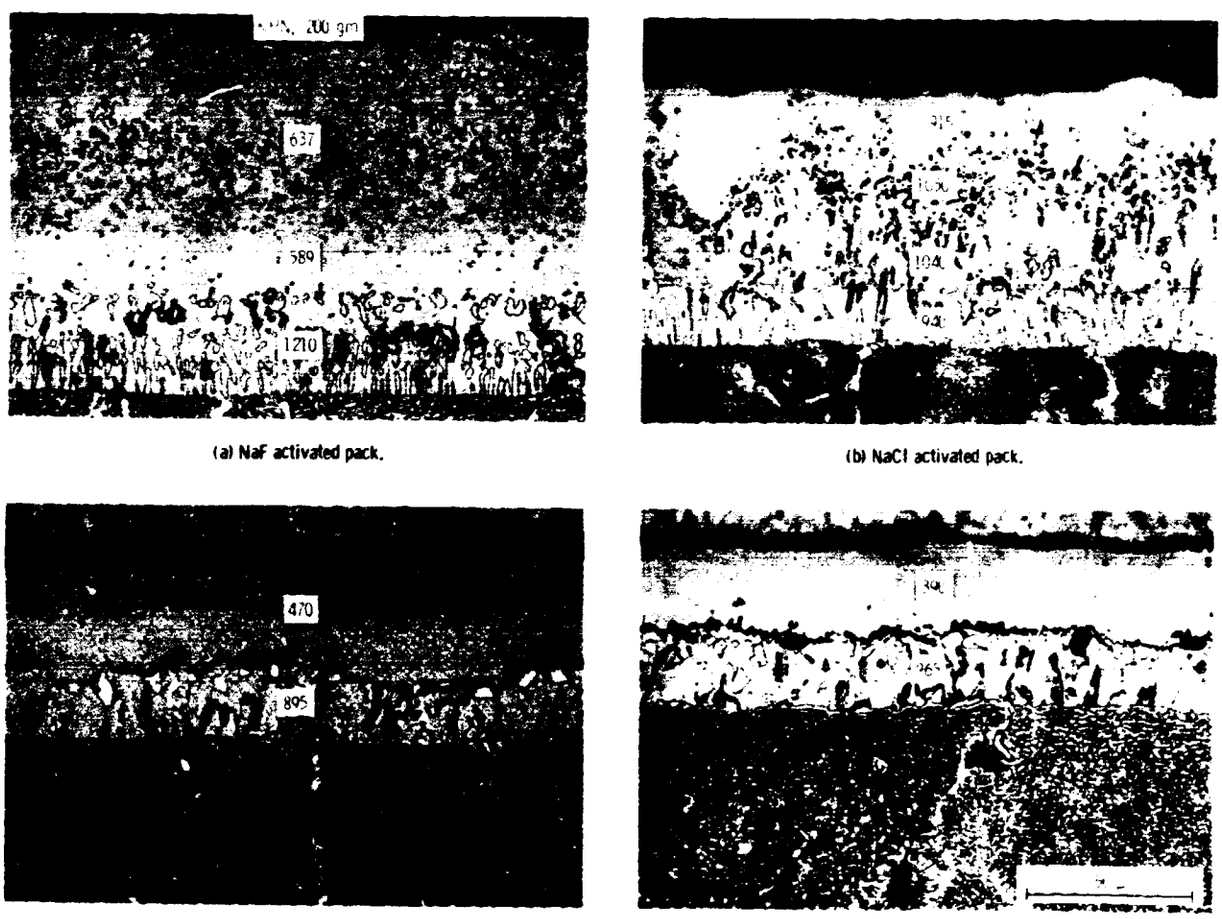

(a) NaF activated pack.

(b) NaCl activated pack.

(c) NaBr activated pack.

(d) NaI activated pack.

Figure 9. - Cross sectional micrographs showing the effect of halogen variation in sodium halide activated 1093° C 16-hour packs.

(a) NH_4F activated pack.

(b) NH_4Cl activated pack.

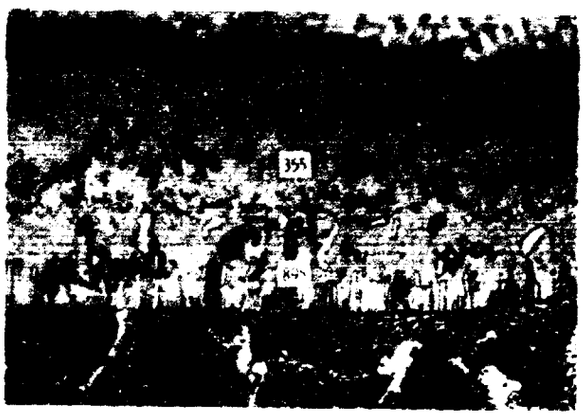

(c) NH_4Br activated pack.

(d) NH_4I activated pack.

Figure 10. - Cross sectional micrographs showing the effect of halogen variation in ammonium halide activated 1093° C, 16-hour packs.

Figure 11. - Cross sectional microstructure of an aluminide coating deposited on IN-100 in a 1 wt % NaBr, 5 wt % Al, 16-hour 1093° C pack.

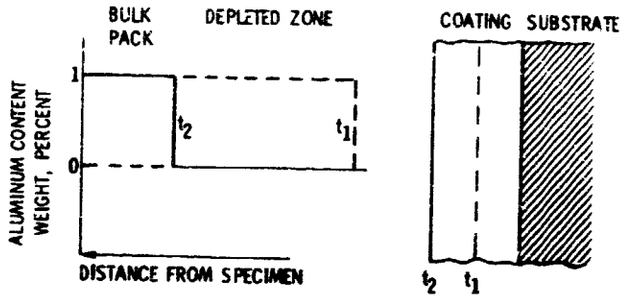

Figure 12. - Idealized depleted zone formation during pack aluminiding. Time, $t_2 > t_1$.

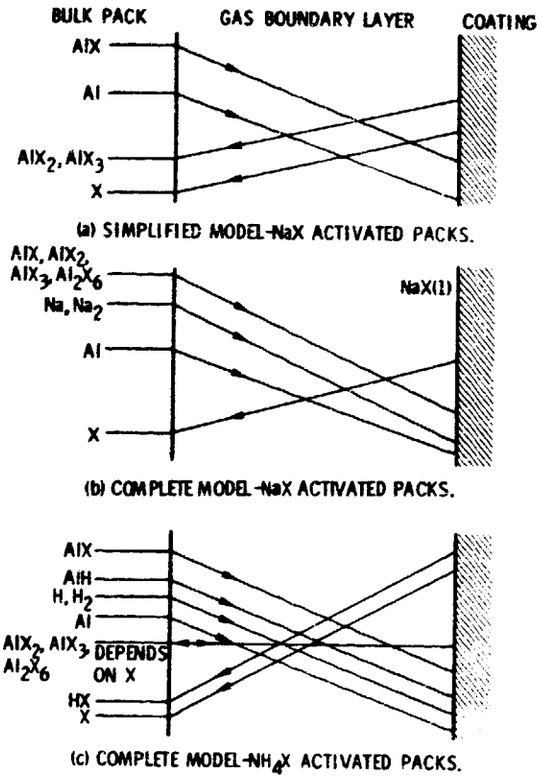

Figure 13. - Schematic showing gas phase diffusion directions during aluminum deposition.

E-7676

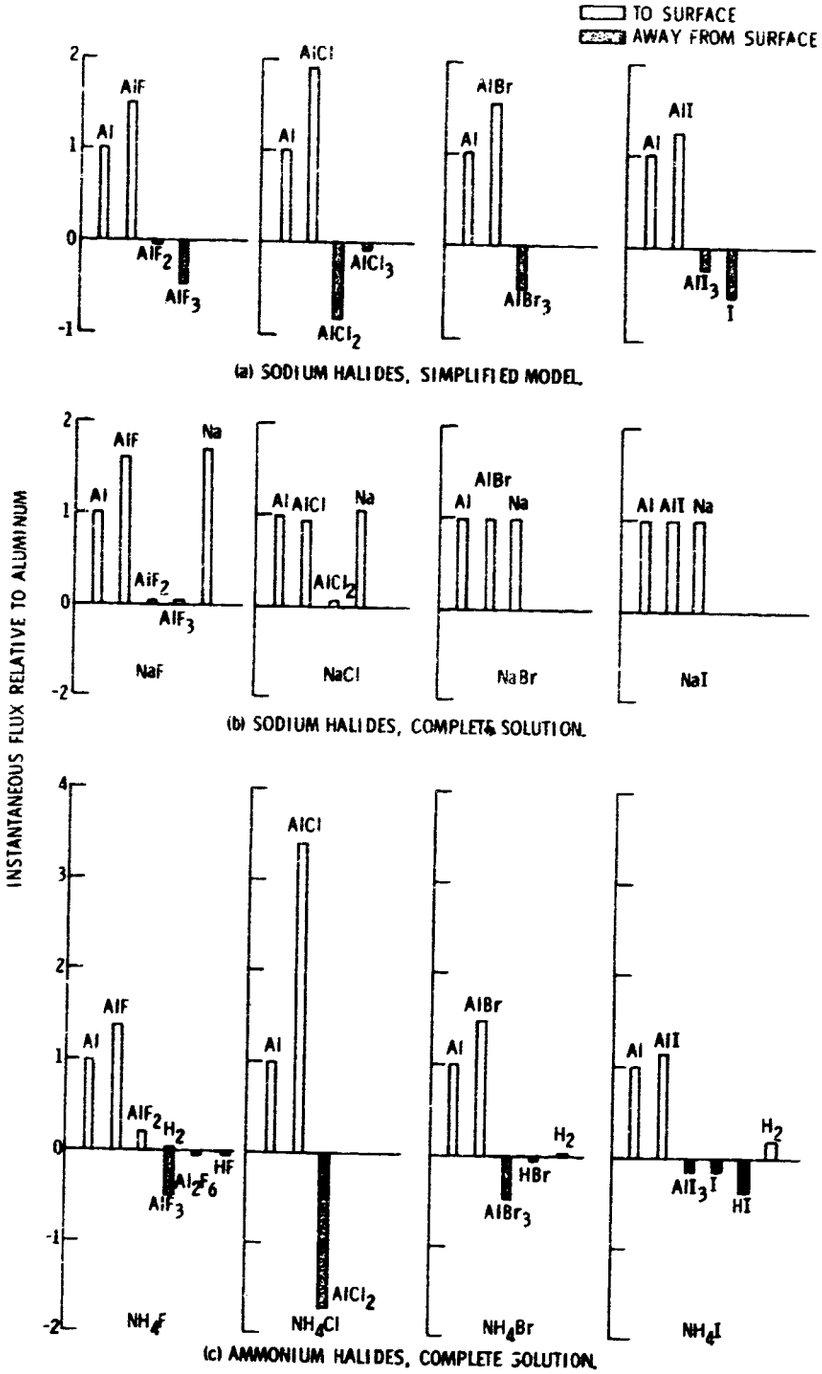

(a) SODIUM HALIDES, SIMPLIFIED MODEL

(b) SODIUM HALIDES, COMPLETE SOLUTION

(c) AMMONIUM HALIDES, COMPLETE SOLUTION

Figure 14. - Instantaneous fluxes of diffusing species relative to net instantaneous aluminum flux. Surface aluminum activity, 0.01; 1 weight % Al; 1093° C packs.

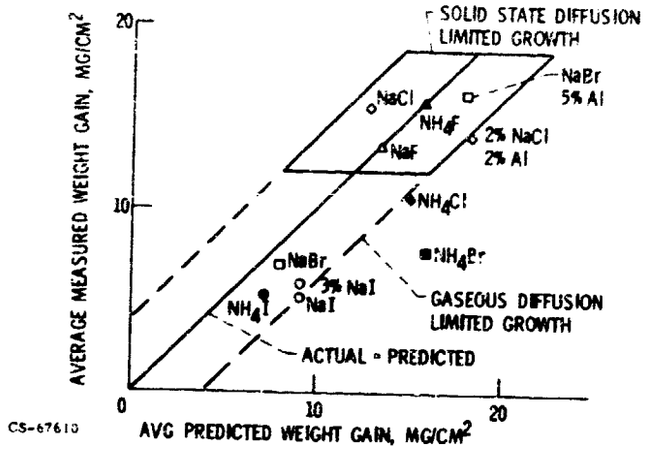

Figure 15. - Comparison of actual and predicted aluminum weight gain for IN-100; 1093° C, 16-hour packs. 1 Weight percent Al and activator unless indicated otherwise.

E-7671

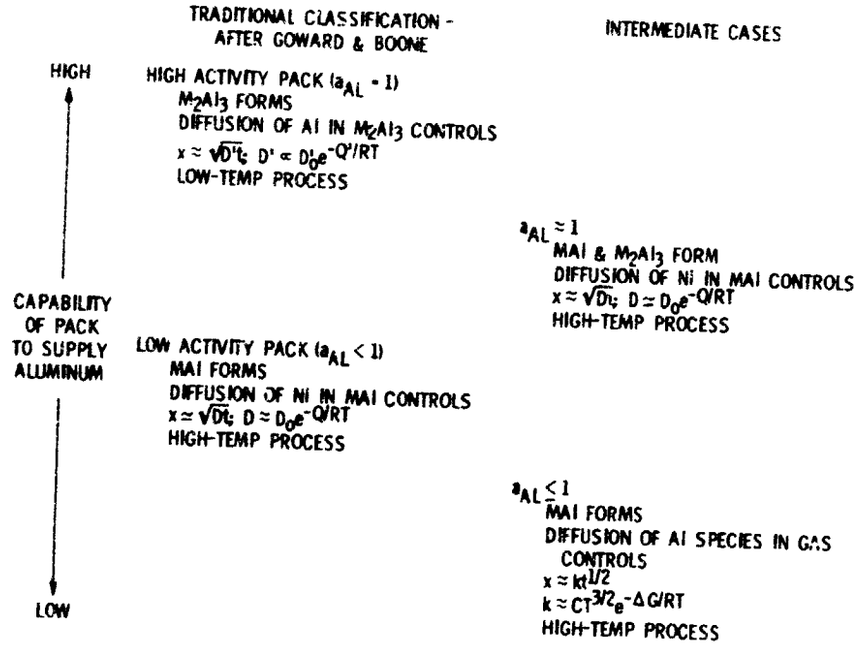

Figure 16. - Proposed expanded classification of aluminide packs.

END

DATE

FILMED

JAN 11 1974